18th International Conference on Structural Mechanics in Reactor Technology (SMiRT 18)
Beijing, China, August 7-12, 2005
SMiRT18-G08-5

INFLUENCE OF A WELDED PIPE WHIP RESTRAINT ON THE CRITICAL CRACK SIZE IN A 90° BEND

Igor Varfolomeyev
Fraunhofer-Institut für Werkstoffmechanik, Freiburg, Germany
Phone: +49 761 5142 - 210, Fax: - 401
E-mail:
Igor.Varfolomeyev@iwm.fhg.de

Wieland Holzer
TÜV Industrie Service GmbH, Munich, Germany
Phone: +49 89 5791 - 2773, Fax: - 2837
E-mail:
Wieland.Holzer@tuev-sued.de

Dieter Beukelmann
TÜV Industrie Service GmbH, Munich, Germany
Phone: +49 89 5791 - 1105, Fax: - 2606
E-mail:
Dieter.Beukelmann@tuev-sued.de

Wolfgang Mayinger
E.ON Kernkraft GmbH, Hanover, Germany
Phone: +49 511 439 - 4501, Fax: - 4377
E-mail:
Wolfgang.Mayinger@eon-energie.com

ABSTRACT

Finite element analyses have been performed to investigate behaviour of postulated cracks in the longitudinal weld of a 90° pipe elbow in the reactor coolant line of a German PWR. At the extrados a pipe whip restraint is welded on the outer surface of the elbow in order to prevent pipe whip for the postulated double-ended rupture. However, this arrangement significantly increases the effort for non-destructive testing (NDT) during in-service inspections. Moreover, weld sections of about 80 mm to 160 mm length cannot be accessed by NDT from outside.

According to the German RSK (Reactor Safety Commission) Guideline, cracks postulated in areas of restricted access for NDT or in non-examinable zones should not cause a catastrophic failure of the reactor coolant line. To assure the safety of the pipe elbow against crack initiation and unstable propagation, numerical stress and crack driving force calculations are carried out taking into account the real geometry of the pipe whip restraint. Both Service Level A Loadings and Service Level D Loadings (e.g. earth quake, plane crash) are investigated. For comparison purposes the same elbow geometry without restraint is analysed. The material J_i value and the slope dJ/da of the measured J_R-curve are employed as criteria for crack initiation and instability.

The results suggest the critical length of a through crack ($2c$) at initiation to be of some 800 mm which is considerably larger than the length of the non-examinable zone. Furthermore, by comparing the slope of the $J_{appl}(2c)$ curve with the material resistance curve, a conclusion can be drawn that no crack instability may occur for any crack size below the length of the pipe whip restraint. The restraint arrangement considerably increases the carrying capacity and residual strength of the elbow.

Keywords: pipe whip restraint, elbow, critical crack size, PWR

 Copyright © 2005 by SMiRT18

1. INTRODUCTION

For pressurized components of power plants or other safety relevant structures it has to be shown that fabrication- or operation-related defects, or postulated initial flaws can not cause failure of the component during its lifetime. As an additional safety margin, the leak-before-break (LBB) criterion is used to assure that global failure of a structure containing a part-through or a through-wall crack is excluded. The LBB condition is fulfilled if the length of the postulated through crack is less than the critical crack length which would lead to global instability. The length of a through crack can be analytically assessed starting from a reasonably assumed initial crack postulate (e.g. small surface defect) and considering its growth under in-service loading. Alternatively, the size of the crack to be evaluated is determined by non-destructive testing (NDT) which is commonly employed during plant inspections.

This paper deals with the safety analysis of the reactor coolant line of a German 1300 MW pressurized water reactor. The component under consideration is a 90° pipe elbow connecting the coolant pipe with the main pump. To prevent possible pipe whip due to a postulated double-ended rupture, a pipe whip restraint is welded on the outer surface of the elbow, at the extrados. The restraint arrangement is beneficial for both the stiffness and the strength of the component; however, it considerably increases the effort for non-destructive testing during in-service inspections of the respective longitudinal weld.

According to the German RSK (Reactor Safety Commission) Guideline (1981), cracks postulated in areas of restricted access for NDT or in non-examinable zones should not cause a catastrophic failure of the reactor coolant line. To assure the safety of the pipe elbow against crack initiation and unstable propagation, numerical stress and fracture mechanics analyses are performed taking into account the real geometry of the pipe whip restraint. Both Service Level A (normal operation) and Service Level D (faulted conditions) loadings are investigated. *J*-integral computations are carried out for through-wall cracks of different length. The material J_i value and the slope dJ/da of the measured J_R-curve are employed as criteria for crack initiation and instability.

The results show that the pipe whip restraint crucially affects the carrying capacity of the elbow, so that no global elbow rupture is expected for a wide range of the crack length well above the size of the non-examinable zone. Furthermore, the effect of taking account of the clad layer on the behaviour of postulated cracks is briefly discussed.

2. COMPONENT GEOMETRY, MATERIAL AND LOADING

The elbow geometry together with the pipe whip restraint is schematically shown in Fig. 1. The component has following dimensions: bend radius R_B = 1125 mm, inner radius of the pipe R_i = 380 mm, wall thickness t = 48 mm. This corresponds with the minimum design thickness for the component. An austenitic clad layer with the thickness of 5 mm is welded on the inner surface of the piping.

The pipe elbow is made of a ferritic steel 20 MnMoNi 55 with the yield strength $R_{p0.2}$ = 371 MPa, the ultimate strength R_m = 513 MPa (16% strain), Young's modulus of elasticity E = 192 GPa, and Poisson's ratio ν = 0.3. According to these data, a multi-linear stress-strain curve was employed in numerical calculations. The clad material (type 1.4550) was assumed to have the yield strength of $R_{p0.2}$ = 240 MPa and a linear hardening behavior with the tangential modulus E_T = 2 GPa. All material data above apply to the operation temperature of about 300°C.

The piping is subjected to internal pressure and reaction forces and moments resulting from weight loads, thermal expansion of the system, restraint conditions, external loads, etc. The reaction forces and moments are referred to a specific nodal point of the piping and are replaced, for the sake of simplicity, by an equivalent global bending moment, M_{eq}, accounting for both in-plane and out-of-plane loads. The moment M_{eq} is then considered as the in-plane load, thus yielding conservative estimates of the crack driving force. The effect of shear forces is accounted for through their contributions in M_{eq}, whereas the impact of the torque loads is omitted. Accordingly, the opening mode deformation (mode I) for crack postulates is considered in this study.

Table 1 summarizes the loads acting on the pipe elbow for both Service Level A and Service Level D conditions, as considered in the paper.

 Copyright © 2005 by SMiRT18

Table 1: Loading conditions and parameters.

Load conditions	Internal pressure, MPa	Equivalent bending moment, kNm
Service level A (in-service loading)	15.8	290
Service level D (faulted conditions, e.g. earth quake, plane crash)	15.8	615

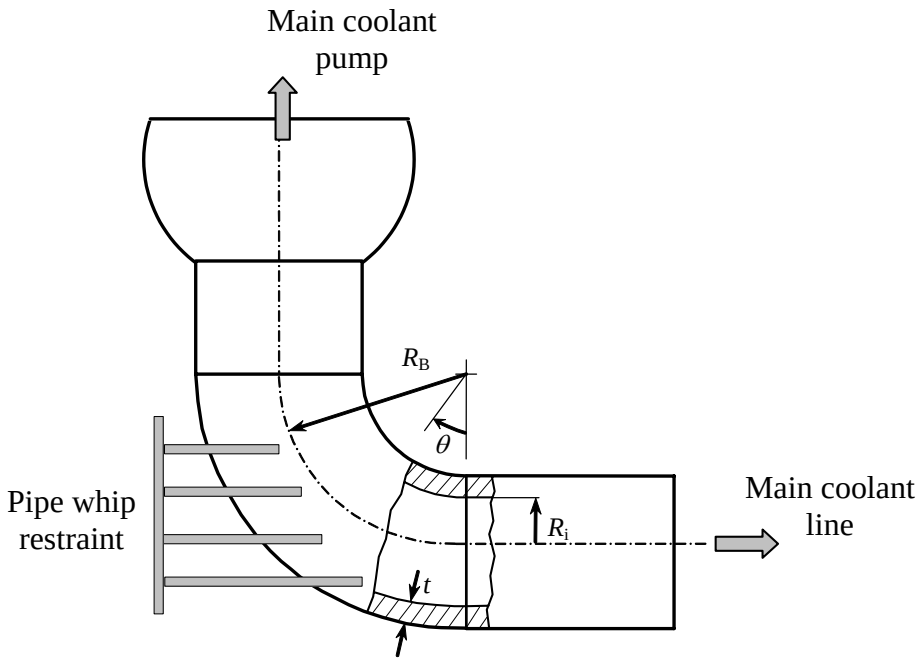

Fig. 1 Schematic of the elbow with the pipe whip restraint.

3. FINITE ELEMENT MODELS AND RESULTS

Numerical modeling of the pipe elbow was performed using the finite element code ABAQUS (2003). Models with different through-wall crack length were investigated. The models used typically consisted of 32000 to 38000 elements and 43000 to 48000 nodes. Both 6-node prism and 8-node brick continuum elements with linear displacement interpolation were employed. In the vicinity of the crack front, 8-node elements were used. Computations of the *J*-integral were performed based on the virtual crack extension method (ABAQUS, 2003).

As an example, Fig. 2 shows a finite element model of the elbow containing a 30.75° long through crack in the extrados. Five element layers (one in the cladding and four in the base material) are used over the wall thickness, so that the *J*-integral is evaluated on 6 locations along the crack front.

3.1 Stress Analyses of the Intact Elbow

First, elastic stress analyses of the component without flaws were carried out to study the influence of the restraint arrangement on the stress distribution in the extrados where crack postulates are to be investigated. Figure 3 compares the hoop stress distribution for the models with and without the pipe whip restraint. The stresses are estimated at the wall center, for the in-service loading conditions (Table 1). The *x*-coordinate represents the arc angle θ (in degrees) measured starting from the lower elbow end (connection to the main coolant line, see Fig. 1).

 Copyright © 2005 by SMiRT18

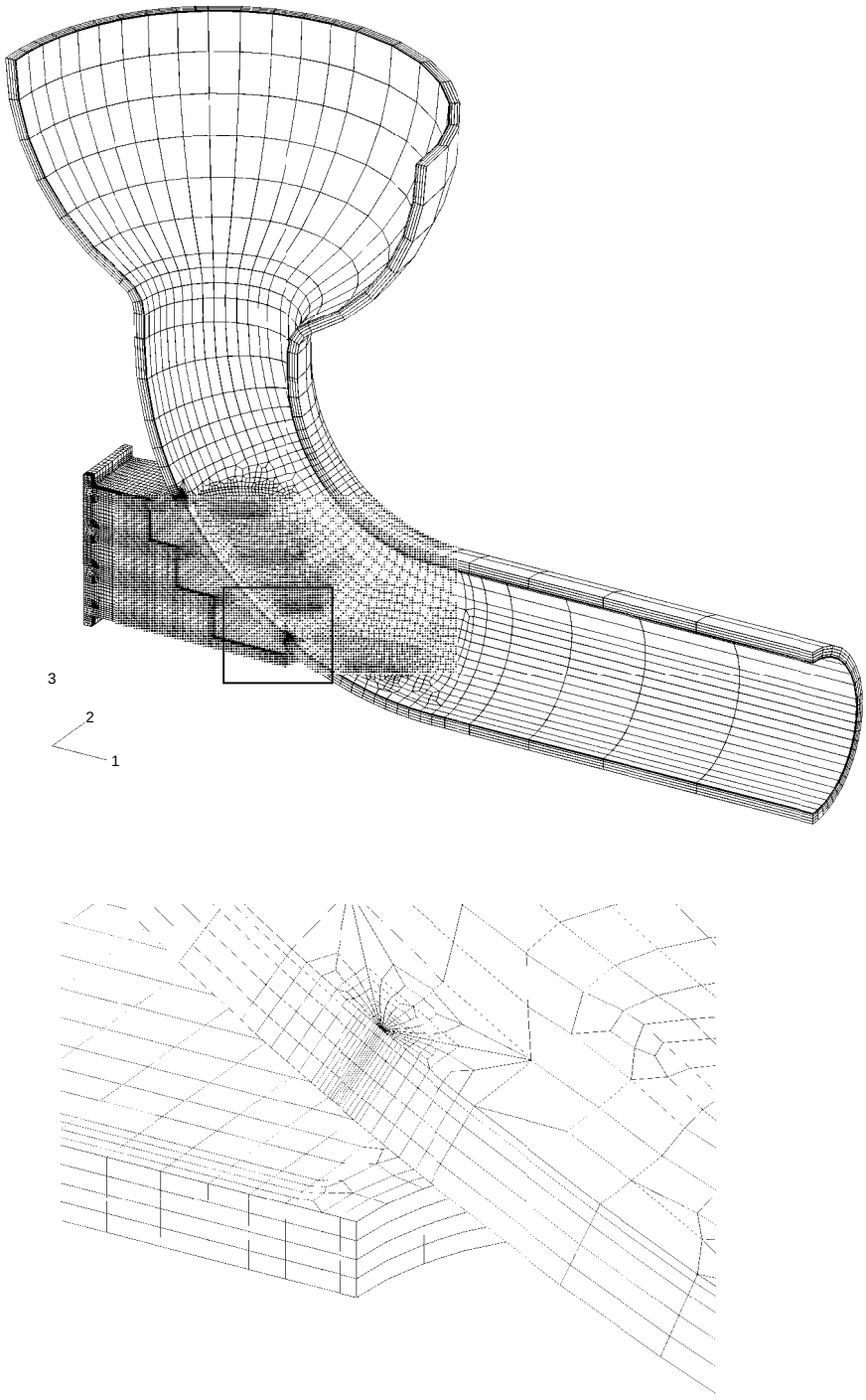

Fig. 2 Finite element model of the elbow with a 30.75° long through crack at the extrados. Lower frame: mesh details near the crack front.

 Copyright © 2005 by SMiRT18

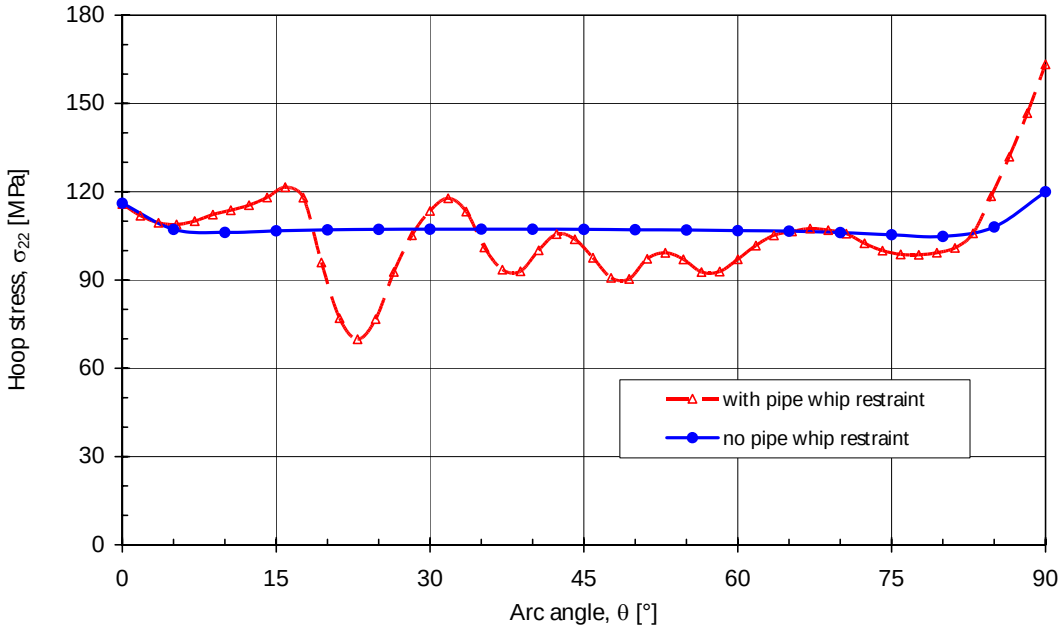

Fig. 3 Hoop stress distribution in the extrados of the elbow with and without pipe whip restraint. Load parameters for in-service conditions.

The restraint arrangement affects the stress distribution mainly around the weld connection zones where some oscillating stress behavior is observed. In the middle part of the elbow (θ = 30° to 60°), the presence of the pipe whip restraint leads to some reduction in the stress magnitude of about 10%. This effect alone would lead to a moderate reduction in the crack driving force for surface flaws. However, due to the stiffness of the restraint arrangement, its influence on the behaviour of through cracks is remarkable, as it is shown in the following section.

3.2 Numerical Analyses of the Cracked Elbow

Fracture mechanics computations were carried out for postulated through-wall cracks at the extrados. The smallest crack in the analyses had an arc length of 2α = 30.75° corresponding with the crack length of $2c$ = 820 mm, as measured along the mean radius of the cross-section in the extrados. The respective finite element model is shown in Fig. 2. The postulated crack is placed symmetrically with respect to the elbow geometry (crack center at θ = 45°), and the crack size is selected such that both crack tips lie just beyond the restraint arrangement, i.e. outside the non-examinable area.

Further crack models were selected to provide the J-integral values and the slope of the $J(2c)$ curve for a crack length close to the critical one. Accordingly, two additional crack sizes with 2α = 54° and 58.5° ($2c$ = 1440 and 1560 mm) were considered. The latter flaw postulates were placed asymmetrically (crack center at θ = 33.75° in both cases). This is because the analyses revealed somewhat higher crack driving force for the crack front approaching the main coolant pipe (as marked by the frame in Fig. 2), so that the crack extension towards the pipe is more likely. Consequently, all numerical results presented below refer to the crack front with the higher values of the crack driving force.

Numerical computations were performed using multi-linear stress-strain curves for the base and clad materials according to the data reported in Section 2. Large strain analysis was employed.

Figure 4 shows the J-integral distribution along the crack front for both in-service load and faulted conditions (Table 1). In the above plot, the position on the crack front is defined by a dimensionless parameter, s/t, where s is the radial distance from the inner surface to the current point.

Despite of a considerable increase in the bending moment when comparing the Service Level A and the Service Level D load cases (Table 1), merely minor differences arise in the crack driving force. This should be attributed to the particular crack position and orientation. Namely, with increasing bending moment (from 290 to

Copyright © 2005 by SMiRT18

615 kNm) the hoop stress distribution in the extrados changes insignificantly: the maximum stress increases by 3.5%, whereas the mean value over the wall remains almost unchanged. At the same time, the maximum hoop stress in the intrados increases by 8%.

Hence, it can be expected that the behavior of a through-wall crack located at the extrados or intrados of a pipe elbow is mainly defined by the value of the internal pressure. This conclusion is in accordance with the numerical results (Siegele *et al*., 1999a) on the leak-before-break analysis for a 50° elbow. In contrast, for crack postulates at the crown, the effect of the bending moment is considerable (Siegele *et al*., 1999b).

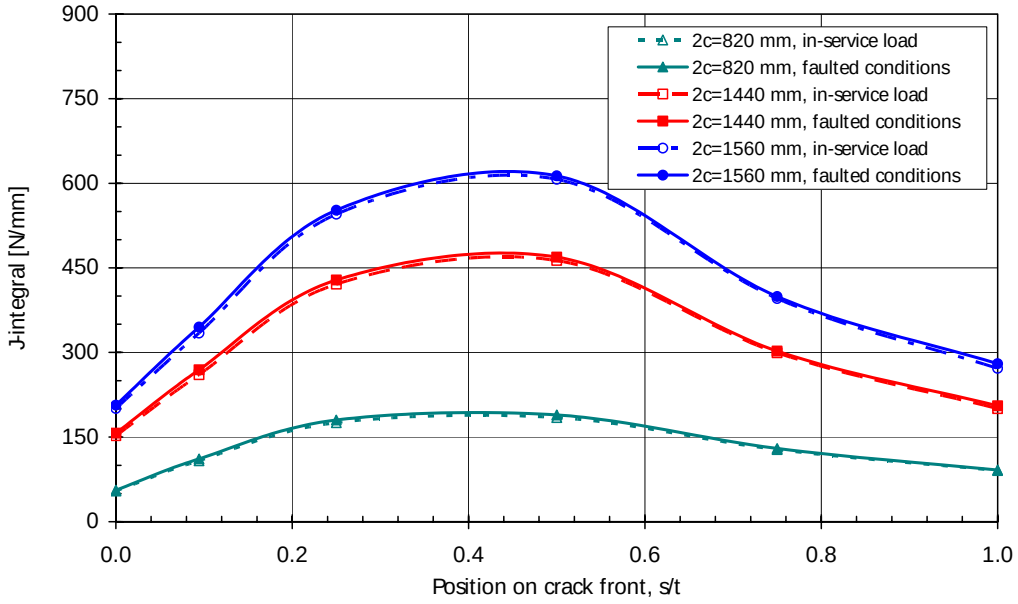

Fig. 4 J-integral along the crack front for two load levels and variable crack length.

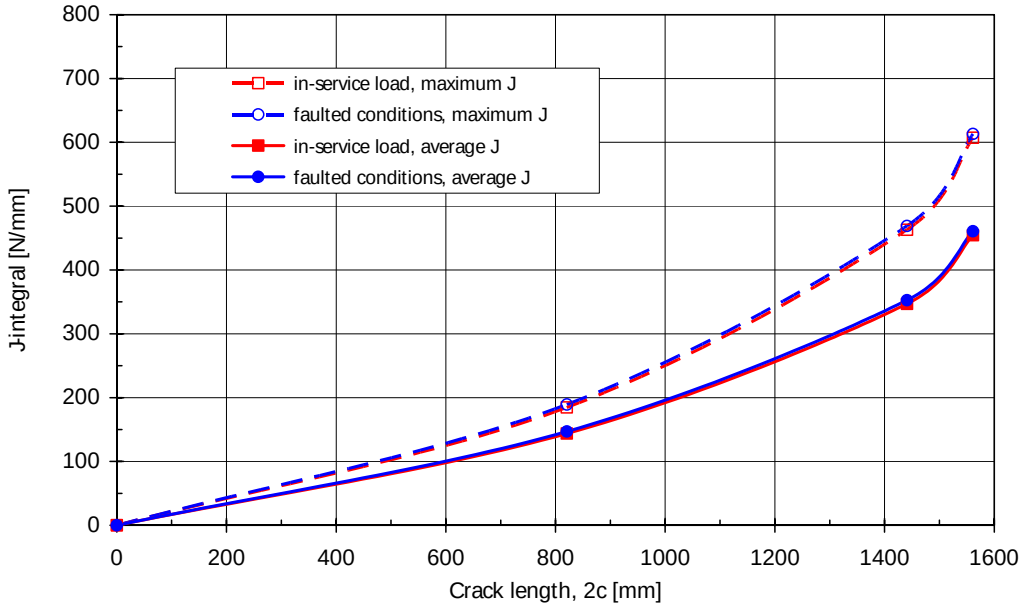

Fig. 5

Copyright © 2005 by SMiRT18

Figure 5 shows the variation of the *J*-integral versus crack length. Both the maximum value of the *J*-integral and its average along the crack front are plotted. The average *J*-value is defined by

$$J_{aver} = \frac{1}{t}\int_0^t J(s)ds\,, \tag{1}$$

and seems to be more appropriate to characterize the behavior of through cracks.

4. ESTIMATES OF THE CRITICAL CRACK LENGTH

To evaluate conditions for the crack initiation and instability, the J_R-curve was measured for the original material of the elbow. For this purpose, two compact tensile specimens with 20% side grooves were tested at temperature of about 300°C using the method of partial unloading. The *J*-integral values up to 440 N/mm and the crack extension, Δa, up to 6 mm were accomplished in the tests. The measured data pairs (J, Δa) were then approximated by a polynomial function with the resulting fit curve shown in Fig. 6.

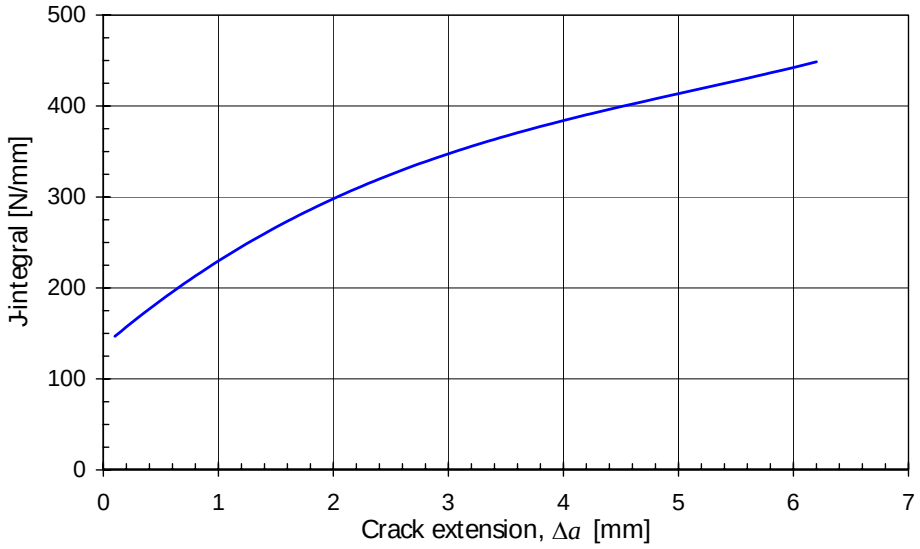

Fig. 6 J resistance curve for the elbow material.

In particular, the measured *J*-integral value at crack initiation was about $J_{0.2}$ = 160 N/mm, whereas the slope of the J_R-curve within its end part, representing the minimum slope for the whole measured curve, was estimated to be at least $(dJ/da)_{mat}$ = 27 N/mm^2.

Comparing the above $J_{0.2}$ value with the computational results (Fig. 5), a conclusion can be drawn that no initiation is achieved for crack postulates in the extrados with the length below 820 mm, i.e. those which can be detected within the area of access by NDT. Herein, the use of both the maximum and the averaged values of the *J*-integral leads to comparable estimates.

Increasing crack length gives rise to the crack driving force and the slope of the applied $J(2c)$ curve. As a criterion for stable crack extension, the following condition is commonly used (e.g. Kanninen and Popelar, 1985):

$$\left(\frac{dJ}{dc}\right)_{appl} < \left(\frac{dJ}{da}\right)_{mat} \tag{2}$$

The calculated $J(2c)$ curves (Fig. 5, averaged values) are compared in Fig. 7 with the minimum slope of the material fracture resistance curve. The latter is indicated by a straight line passing through the end point of the J_{appl} curve for the faulted conditions. For the largest of the considered crack postulates, $2c$ = 1560 mm, the stability criterion, Eq. (2), is still fulfilled. By extrapolating the J_{appl} curve (dotted line in Fig. 7), the critical crack length slightly above 1600 mm can be found.

 Copyright © 2005 by SMiRT18

In some cases it may be desirable to neglect effects of cladding on the structural behavior. This helps to optimize the modeling effort and reduce computer time, but also yields conservative estimates of the crack driving force (e.g. Siegele *et al*., 1999a). Figure 7 shows *J*-integral estimates for the considered crack postulates in the component with no clad layer. The respective *J* values are 20% to 30% higher than those for the elbow with cladding, however, the critical crack size (between 1560 and 1600 mm) appears to be insignificantly smaller.

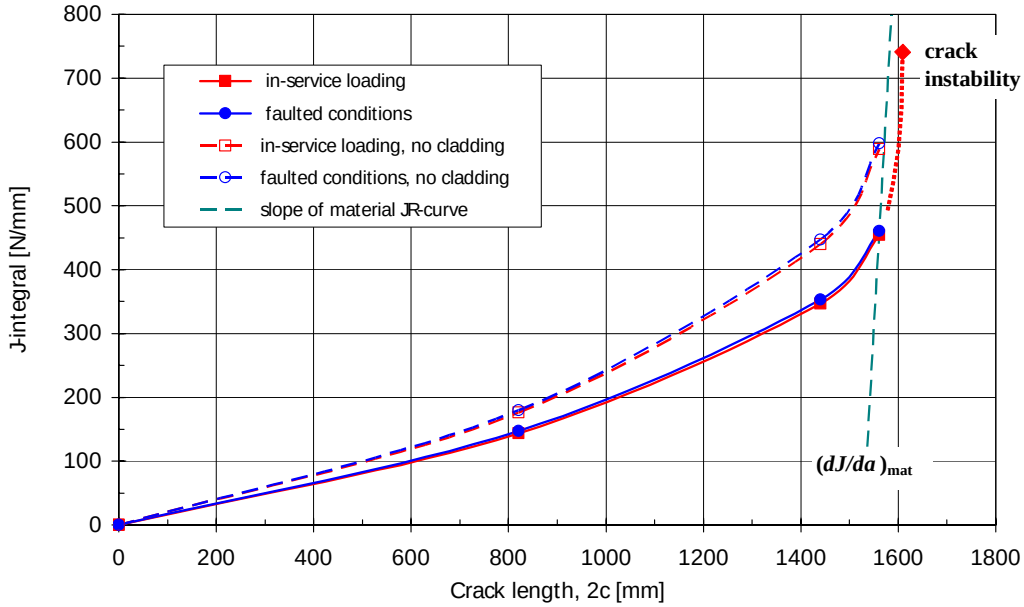

Fig. 7 Estimation of the critical crack size.

Finally, Fig. 8 compares results of the *J*-integral analyses for the elbow with and without the pipe whip restraint, at in-service loading. A slight difference in the results is found for crack lengths below 300 mm. For longer cracks, however, taking no account of the restraint arrangement would lead to a significant overestimation of the *J*-integral: so, the crack initiation would be predicted for a crack length about 420 mm which is almost a half of that with the pipe whip restraint being considered.

Copyright © 2005 by SMiRT18

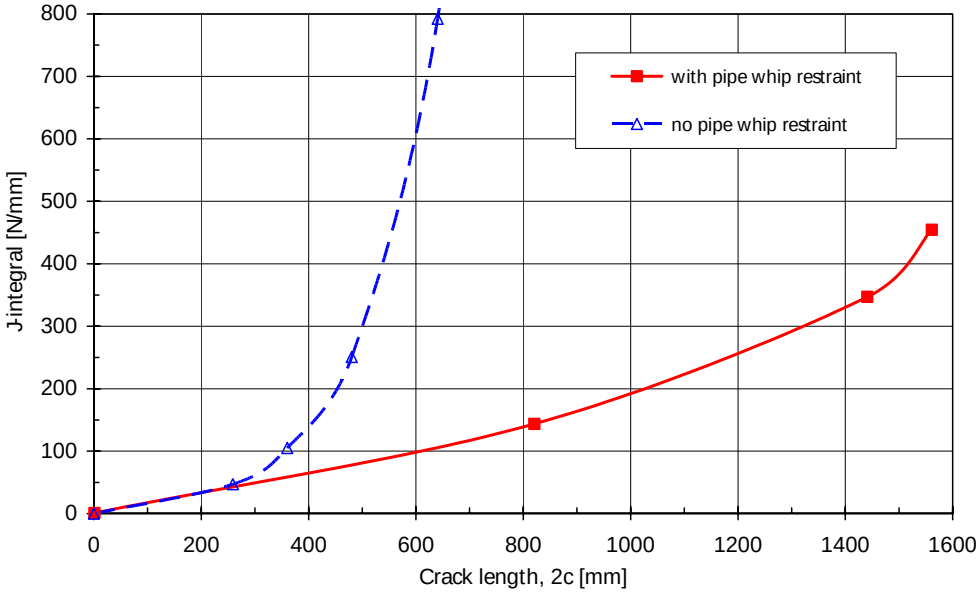

Fig. 8 Comparison of the crack driving force for the component with and without pipe whip restraint, at in-service loading.

Material data (such as $J_{0.2}$, the slope of the J_R-curve) used in the assessment of cracked components are usually determined on small test specimens. The transferability of the test data from specimens to the component has to be proven, e.g. by considering the corresponding stress state at the crack tip. Different constraint parameters can be employed to relate the stress fields in the specimen with that in the component. For instance, the stress triaxiality factor, *h*, defined as the ratio of the hydrostatic to the equivalent Mises stress is often used (Brocks and Schmitt, 1995). Generally, the J_R-curve measured on a specimen with high constraint (large triaxiality factor) conservatively describes the crack behavior in another specimen or component with lower constraint level.

Figure 9 shows the variation of the *h* parameter versus applied load (*J*-integral) for the elbow with a 1560 mm long through crack, as well as for the C(T)25 specimen used in the J_R-curve measurements. In both cases, the increase in the crack tip loading results in the decreasing *h* factor, which can be attributed to the growing plastic zone in the ligament. In the C(T) specimen, the stress triaxiality factor varies between 2.5 and 2.2 for the *J* values corresponding to the crack initiation ($J_{0.2}$ = 160 N/mm) and to the end part of the measured J_R-curve (*J* = 440 N/mm). Within the same range of the *J*-integral, the stress triaxiality factor for the cracked elbow changes from 2.1 to 1.9, thus remaining sufficiently lower than for the test specimen. Consequently, the application of the J_R-curve measured on the C(T) specimens yields conservative predictions of the initiation and instability for postulated through-wall cracks in the elbow.

Copyright © 2005 by SMiRT18

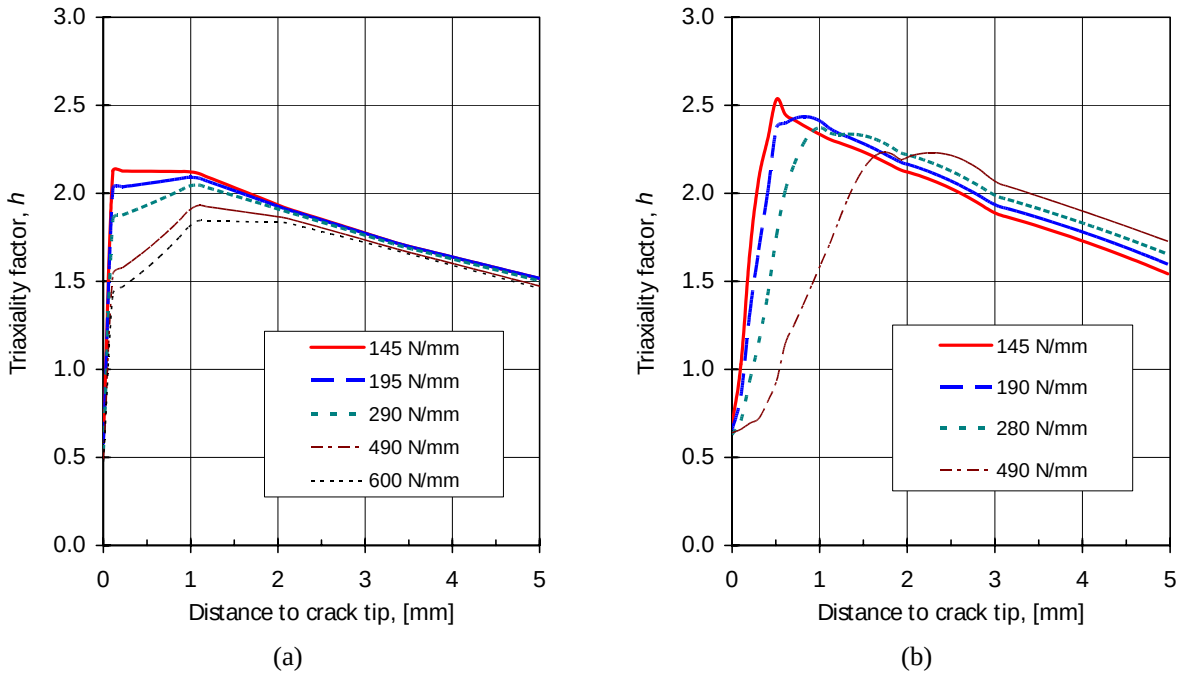

Fig. 9 *Stress triaxiality ahead of the crack front at different values of the J-integral: (a) through-wall crack in the elbow (2c = 1560 mm); (b) C(T)25 side grooved specimen.*

5. CONCLUSIONS

Fracture mechanics analyses were performed for a component of the reactor coolant line of a pressurized water reactor. The considered 90° elbow connecting the coolant pipe with the main pump has a restraint arrangement to prevent possible pipe whip due to a postulated double-ended rupture. The pipe whip restraint is welded at the outer surface of the extrados, thus limiting the area of access for NDT during in-service inspections of the respective longitudinal weld.

According to the German RSK (Reactor Safety Commission) Guideline (1981), cracks postulated in areas of restricted access for NDT or in non-examinable zones should not cause a catastrophic failure of the reactor coolant line. To demonstrate the safety of the elbow against crack initiation and unstable propagation, *J*-integral computations were numerically performed for postulated through-wall cracks of different length. Both in-service and faulted (due to earth quake, plane crash, etc.) loading conditions were investigated.

The results suggest the crack length at ductile initiation to be about 820 mm (30° arc length) which is significantly larger that the size of the area of limited access by NDT, owing to the restraint arrangement. Comparing the slope of the applied $J(2c)$ curve with the slope of the J_R-curve measured on the original elbow material using standard C(T) side grooved specimens, the critical flaw size corresponding to unstable crack propagation is found to be some 1600 mm. An examination of the stress fields and constraint parameters (stress triaxiality) for cracks in the elbow and in the test specimen revealed that the above estimate of the critical crack size is fairly conservative. Therefore, no global rupture of the component is expected for a wide range of the crack length well above the size of the non-examinable zone.

REFERENCES

ABAQUS (2003), User's Manual, Version 6.4, ABAQUS, Inc.

Brocks, W. and Schmitt, W. (1995), The second parameter in J-R curves: constraint or triaxiality? In *Constraint Effects in Fracture: Theory and Applications*, Kirk, M. and Bakker, A., Eds., ASTM STP 1244, American Society for Testing and Materials, Philadelphia, pp. 209-231.

Kanninen, M.F. and Popelar, C.H. (1985), *Advanced Fracture Mechanics*, Oxford University Press, New York, Clarendon Press, Oxford.

 Copyright © 2005 by SMiRT18

RSK Guideline (1981), RSK Guidelines for Pressurized Water Reactors, Original Version (3rd Edition of 14.10.81) with amendments of 15.11.96, German Reactor Safety Commission (in German).

Siegele, D., Varfolomeyev, I., Hodulak, L, and Nagel, G. (1999a). Investigations to leak-before-break behaviour of a main coolant pipe, Proceedings 25th MPA-Seminar, Stuttgart, Oct. 1999, pp. 3.1-3.14.

Siegele, D., Varfolomeyev, I., and Nagel, G. (1999b). Leak-before-break analysis of a pipe elbow using fracture mechanics concepts. Proceedings 3rd Int. Conference *"Pipelines Safety"*, Moscow, Sept. 1999, Vol. 4, pp. 39-51.

 Copyright © 2005 by SMiRT18